SEPTEMBER 2011 | VOLUME V | ISSUE IX

Qpedia

IN THIS ISSUE

Qpedia

SUBSCRIBE ON LINE AT:
www.qats.com/qpedia

Advanced Thermal Solutions is a leading engineering and manufacturing company supplying complete thermal and mechanical packaging solutions from analysis and testing to final production. ATS provides a wide range of air and liquid cooling solutions, laboratory-quality thermal instrumentation, along with thermal design consulting services and training. Each article within Qpedia is meticulously researched and written by ATS' engineering staff and contributing partners. For more information about Advanced Thermal Solutions, Inc., please visit www.qats.com or call 781-769-2800.

EDITOR
KAVEH AZAR, Ph.D.

President & CEO,
Advanced Thermal Solutions, Inc.

MANAGING EDITOR
BAHMAN TAVASSOLI, Ph.D.

Chief Technology Officer,
Advanced Thermal Solutions, Inc.

NORTH AMERICA
ADVANCED THERMAL SOLUTIONS, INC.

89-27 Access Road Norwood, MA 02062 USA
T: 781.769.2800 | F: 781.769.9979 | www.qats.com

EUROPE
ADVANCED THERMAL SOLUTIONS, B.V.

De Nieuwe Vaart 50 | 1401 GS Bussum
The Netherlands
T: +31 (0) 3569 84715 | F: +31 (0) 3569 21294
www.qats-europe.com

ADVERTISING
TO PLACE AN AD IN QPEDIA:

Contact John O' Day at 781.949.2521

Qpedia was launched in 2007 as a technology eMagazine focused on the thermal management of electronics. It is designed as a resource to help the engineering community solve the most challenging thermal problems.

The eMagazine is published monthly and distributed at no charge to over 17,000 engineers worldwide. Qpedia is also available online or for download at www.qats.com/qpedia.

Qpedia's editorial team includes ATS' President & CEO, Kaveh Azar, Ph.D., and Bahman Tavassoli, Ph.D., the company's chief technologist. Both Azar and Tavassoli are internationally recognized experts in the thermal management of electronics.

For more information on how you can generate awareness about your company or products, contact John O' Day at 781.949.2521.

Qpedia

Features

Qpedia

Volumes 1 - 3 Now Available in Hardcover Books

Advanced Thermal Solutions, Inc. (ATS) now offers the complete editorial contents of its widely-read Qpedia Thermal eMagazine in three hardbound volumes. The books provide an expert resource for design engineers,engineering managers, and others who want to learn more about the theories and applications of electronics thermal management. The three volume set contains nearly 150 in-depth articles, researched and written by veteran engineers. They address the most critical areas of electronics cooling, with a wide spectrum of topics and thorough technical explanation.

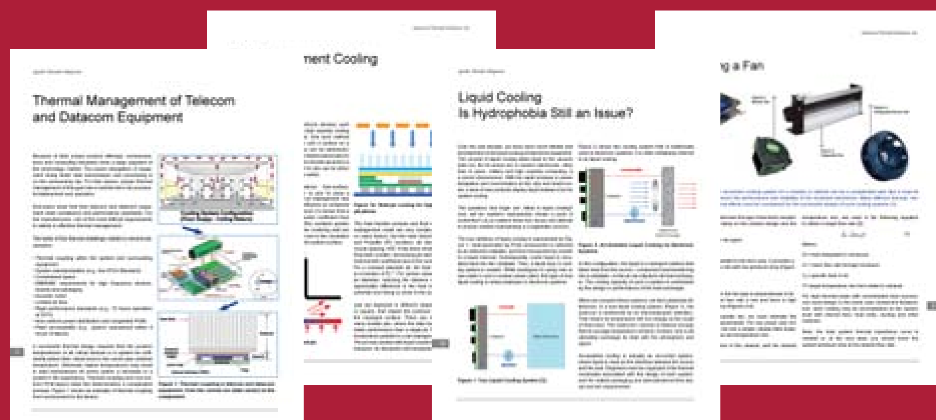

Books Available Individually, or in Book Sets at a Discount Price.

Click the QR symbol to order now

CFD Simulation of Jet Impingement

Jet impingement is one of the most efficient solutions for cooling hot electronic devices, as it can create a very high heat transfer rate on an impacting surface. As the power density of modern chips keeps increasing, using jets as a thermal management method shows great potential, even though its implementation is more complicated than forced air and liquid cooling. Experimental and numerical investigations of flow and heat transfer characteristics, under single or multiple impinging jets, have remained a very dynamic research area in the past two decades. Most electronic cooling applications for impinging jets are focused on studying the turbulent flow in the area downstream of the nozzle and predicting the local and average heat transfer coefficients on the impacting surface. Modeling of turbulent flows presents the greatest challenge for rapidly and accurately predicting impingement heat transfer, even under a single round jet. For jet impingement, the nozzle geometry, jet-to- surface spacing, jet-to-jet spacing, cross flow, operating conditions, etc. all contribute to flow distribution and heat transfer. For numerical simulation of impingement jets, researchers have tried different turbulence models, such as k-ε, k-ω, Reynolds stress models, algebraic stress models, and Menter shear stress transport (SST), etc., although no single model has been universally accepted to be superior to other models in all circumstances. Some turbulent models have been proven to be useful to predict impingement flow and heat transfer within a certain measure of accuracy. This article presents some recent CFD simulation work on impingement jets.

Khan et al. [1] used ANSYS workbench CFX as a CFD tool to numerically study the submerged jet and compared the numerical results to existing experimental measurements. They compared the performance of the k-ε, k-ω, and Menter shear stress transport (SST) turbulence models and found the SST model provided most accurate results.

In the Khan et al. study, the test results of Hammad and Milanovic [2] were used as a benchmark for a CFD simulation comparison. Figure 1 shows the jet impingement experimental setup of Hammad and Milanovic. The schematic of the test section, including tank and pipe, is shown in Figure 2. The tank is made of a clear, cast acrylic to enable the imaging apparatus to take pictures of the particles by Particle Image Velocimetry (PIV) system. Its diameter is 101.6 mm and its height is 279 mm. The jet was created by using a stainless steel pipe. The pipe's diameter is 6.35 mm and its length is 711.2 mm. The flow at pipe's exit is a fully developed jet. In both the test and CFD simulation, water at 30°C was used as a working fluid. The average velocity of the jet was maintained at 2.01 m/s and the flow Reynolds number was 15895.

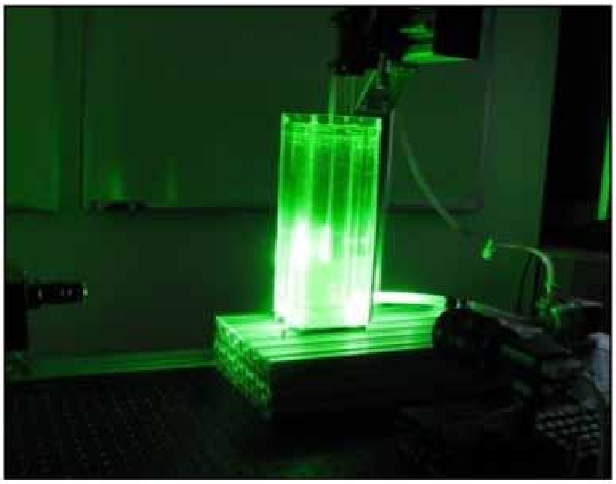

Figure 1. Experimental Setup [2]

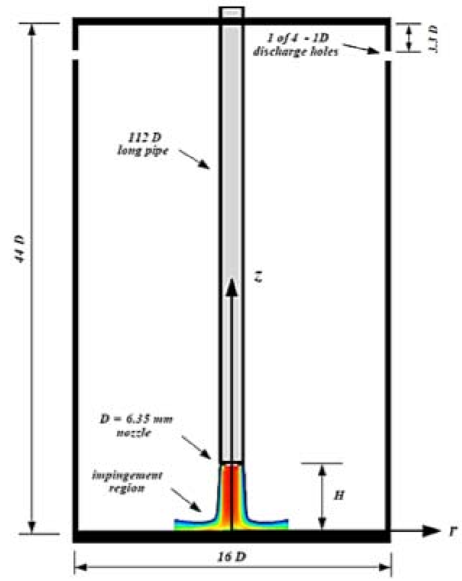

Figure 2. Test Section Schematic [2]

In the CFD simulation of Khan et al. [1], only one-quarter of the tank and pipe is modeled due to the symmetry of the studied domain. Figure 3 illustrates a mesh that was generated to discretize the flow domain of the model. Figure 4 shows the calculated velocity UZ contour plot.

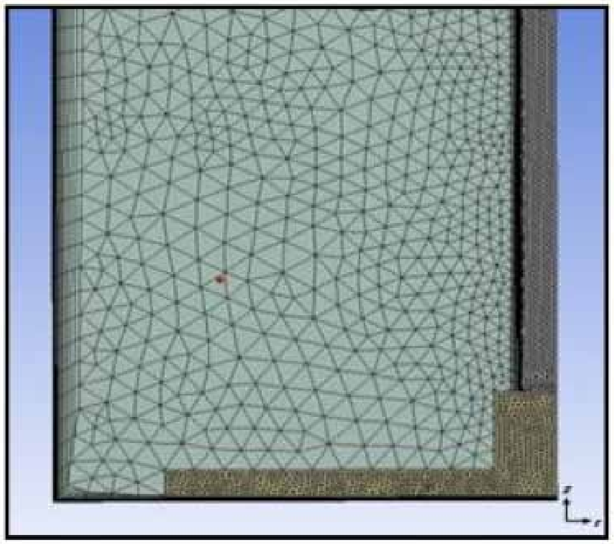

Figure 3. Multi Region Mesh [1]

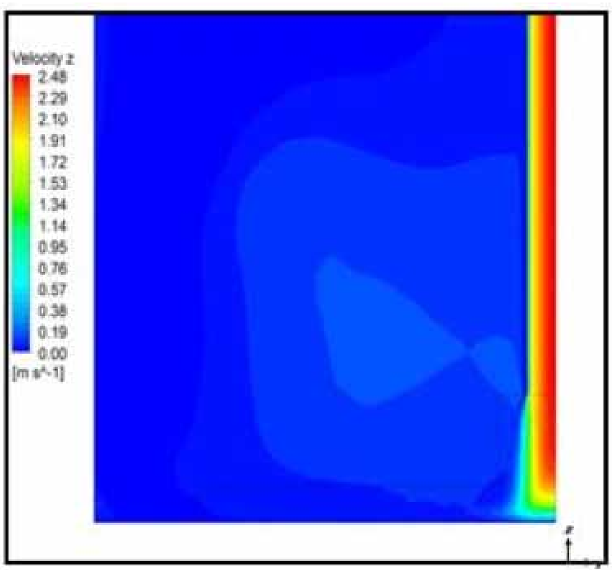

Figure 4. Velocity UZ Contour Plot [1]

Figure 5 shows a view of the mean velocity field in the impingement and the wall-jet regions for separation distance H/D=2 within the measurement domain r/D and z/D. In Table 1, Khan et al. show the percent error from five selected points along the five lines with z/D=0.075 and 0.852. The axial velocity U_z and U_r values were extracted from PIV and CFD data at each point and normalized with U_c=2.48 m/s.

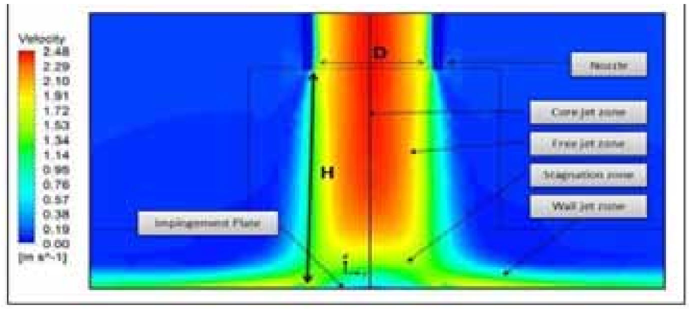

Figure 5. Impingement Jet Velocity Profile for H/D=2 [1]

	Axial velocities comparision at different z/D						Radial velocities comparision at different z/D					
Location	0.075			0.852			0.075			0.852		
r/D	PIV	CFD	error %	PIV	CFD	Error %	PIV	CFD	error %	PIV	CFD	Error %
1.79	0.071	0.056	21.0	0.087	0.079	8.9	0.463	0.564	22.0	0.031	0.032	4.1
1.32	0.081	0.063	21.8	0.075	0.074	1.4	0.531	0.424	20.2	0.015	0.016	4.9
0.71	0.428	0.326	24.0	0.177	0.194	9.6	1.120	1.368	16.9	0.014	0.014	2.0
0.39	0.758	0.471	37.9	1.697	1.716	1.1	0.922	1.023	10.9	0.059	0.055	6.2
0.08	0.852	0.553	35.0	2.332	2.378	2.0	0.206	0.239	16.2	0.034	0.033	3.6
Average Error %			27.9			4.6			17.2			4.2

Table 1. Error Analysis for H/D=2 Case [1]

In the Khan et al. study, a good correlation was shown both qualitatively and quantitatively for both radial and axial velocity profiles in most areas. However, the axial and radial velocity, at a small distance from the impingement plate z/D=0.075, shows a variance that was notably different in comparison with the PIV experimental data. This was due to the turbulence modeling complexity at the stagnation region and near the plate. Khan et al. think the relatively larger percentage of error at the near plate region was attributable to a variety of reasons, such as the numerical schemes and mathematical models used, mesh construction, boundary conditions set up and wall treatment function. This variance decreases as the z/D value increases.

Narumanchi et al. [3] conducted CFD simulation of water by using commercial CFD software Fluent on different jet configurations, such as free-surface jet, submerged jet and confined jet. They compared their numerical results with other researchers' experimental results. The different jet configurations are illustrated in Figure 6.

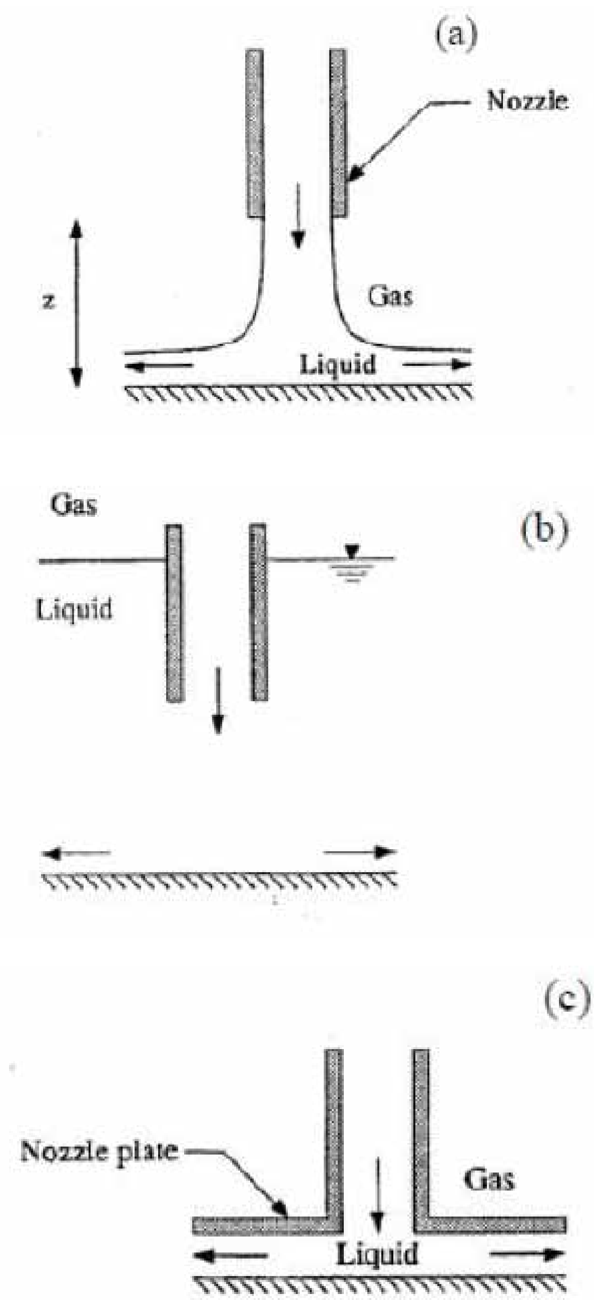

Figure 6. Different Jet Impingement Configurations:
(a) Free-surface Jet, (b) Submerged Jet, (c) Confined Jet [4]

In Narumanchi et al. simulations, they found no single turbulence model yields results that match experimental data for different types of problems and a wide range of Reynolds numbers. The k-ω model is the most suitable model for this class of impinging jet flows. Hence, for all the results reported in their study, they employed the standard k-ω turbulence model with the enhanced wall treatment. For the free-surface jets, the steady- state implicit volume-of-fluid method [5] is used. In this methodology, they performed a two-phase (air and water) simulation, and the interface between the phases is tracked. Figure 7 shows the domain and representative velocity contours with free-surface jets. The simulation uses Womac et al. [6] free-surface jet experimental configuration.

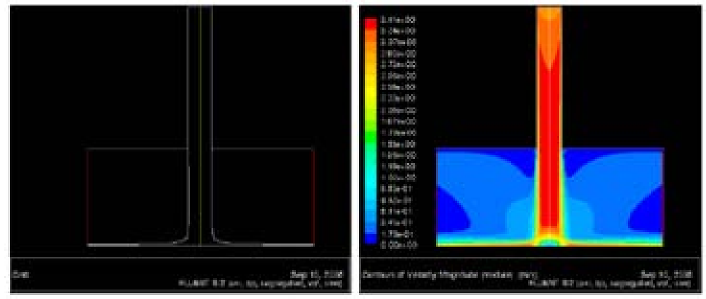

Figure 7. Free-surface Jet
(Womac et al. [6]) Configuration and Velocity Profile [3]

Figure 8 shows the domain and representative velocity contours with submerged jets. The simulation uses the Womac et al. [6] submerged jet experimental configuration.

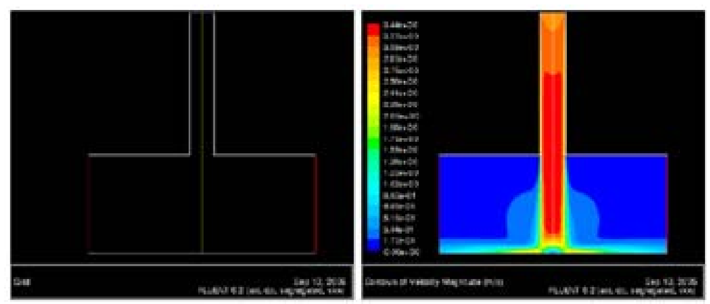

Figure 8. Submerged Jet
(Womac et al. [6]) Configuration and Velocity Profile [3]

Figure 9 shows the domain and representative velocity contours with confined jets. The simulation uses the Garimella and Rice [7] confined jet experimental configuration.

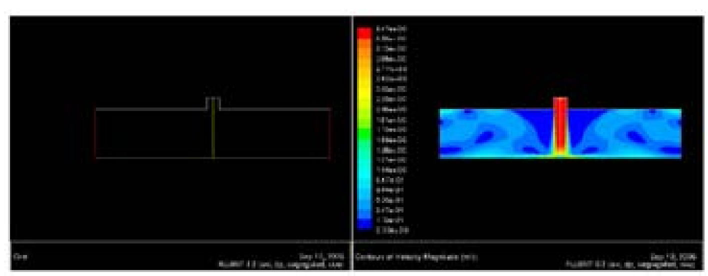

Figure 9. Confined Jet
(Garimella and Rice [7]) Configuration and Velocity Profile [3]

Configuration	Problem parameters	h_{avg} from correlations (W/m^2K)	h_{avg} from CFD (FLUENT) (W/m^2K)	% difference between FLUENT and correlation
Single circular submerged jet (Womac et al. [5])	v = 3 m/s, d = 3.1 mm, D = 14.3 mm, S_{np} = 4d, **Re_d = 9,300**	27,300	26,400	3
	v = 15 m/s, **Re_d = 46,400**	69,300	81,400	16
Single circular free-surface jet (Womac et al. [5])	v = 1 m/s, d = 3.1 mm, D = 14.3 mm, S_{np} = 4d, **Re_d = 3,100**	11,500	14,000	20
	v = 3 m/s, **Re_d = 9,300**	19,600	22,500	14
	v = 15 m/s, **Re_d = 46,400**	45,700	61,000	29
Single circular submerged and confined jet (Garimella and Rice [11])	v = 1.3 m/s, d = 3.2mm, D = 11.3 mm, S_{np} = 4d, **Re_d = 4,100**	18,300	19,200	5
	v = 3.3 m/s, **Re_d = 10,300**	34,800	34,800	0
	v = 7.0 m/s, **Re_d = 22,100**	59,100	54,500	8

Table 2. Average Heat Transfer Coefficient Comparison Between Experimental Results and CFD Simulation Results [3]

Table 2 shows the comparison of the average heat transfer coefficient between the experimental results and the Fluent CFD simulation results. For single, circular submerged jet configurations (Womac et al. [6]), a reasonable match (within 20%) exists with experimental data (obtained from correlations) over a wide range of Reynolds numbers. For the confined jet configuration (Garimella and Rice [7]), again a good match is obtained between CFD predictions and experimental data (within 10%) over a wide range of Reynolds numbers. However, for single free-surface jets (Womac et al. [6]), the discrepancy between CFD predictions and experimental can be as much as 30% for the high Reynolds number cases. Narumanchi et al. think that the shape of the free surface and the thickness of the liquid film are not being captured accurately at elevated Reynolds numbers for free-surface jet.

For numerical simulation of impingement jets, because the fluid mechanics and heat transfer cannot be represented by current turbulence models, all turbulence models have shown advantages and drawbacks on catching the intrinsic nature of jet impingement flow. There is no universally accepted model for modeling the jet impingement flow in all applications. In summary, as this article shows, Khan et al. have had some success on modeling the submerged jet by using the SST turbulence model, while Narumanchi et al. prefer to use the k-ω turbulence model to study the free-surface jet, submerged jet and confined jet.

All these models can provide reasonable simulation results within a certain accuracy, if the model is appropriate for the application. If the model is inappropriate for the application, a large error will be introduced. Future advancements on turbulence modeling will help to close the gap between simulation and reality. For now, the use of CFD simulations of jet impingement has to be backed by verification of the experimental results.

References:

1. Khan, F. A., Milanovic, I., and Hammad, K., "CFD Modeling of Submerged Impinging Jets with Various Separation Distances", Proceedings of the 2011 ASEE Northeast Section Annual Conference, University of Hartford, April, 2011.

2. Hammad, K. J. , and Milanovic, I., "Flow Structure in the Near Wall Region of a Submerged Impinging Jet," ASME fluids Engineering Division summer meeting, Paper 78318, Veil, CO, 2009.

3. Narumanchi, S. V. j., Hassani, V., and Bharathan, D., "Modeling Single-Phase and Boiling Liquid Jet Impingement Cooling in Power Electronics", Technical Report, NREL/TP-540-38787, December 2005.

4. Li, C.-Y. and Garimella, S.V., 2001, "Prandtl-number Effects and Generalized Correlations for Confined and Submerged Jet Impingement", International Journal of Heat and Mass Transfer, 44, pp. 3471-3480.

5. Fluent. User's Guide

6. Womac, D. J., Ramadhyani, S., and Incropera, F. P., 1993, "Correlating Equations for Impingement Cooling of Small Heat sources with Single Circular Liquid Jets", ASME Journal of Heat Transfer, 115, pp. 106-115.

7. Garimella, S. V. and Rice, R.A., 1995, "Confined and Submerged Liquid Jet Impingement Heat Transfer", ASME Journal of Heat Transfer, 117, pp. 871-877.

Getting the Most Out of Your Heat Sink Design:

An Overview of the Parameters Which Influence Your Design

The design of a heat sink needs to be based upon a holistic approach to derive the most satisfactory result possible. Heat sinks are widely used as the primary means of heat transfer from a component to the environmental air. It is, relatively, one of the cheapest cooling methods available on the market, has a high reliability and can be easy to implement. In the past, the heat flux limit achievable with liquid cooled system could be achieved with air cooled systems though advancements in the design of heat sinks [1].

Some of the thermal resistances in the design of a heat sink are shown in Figure 1, which are, namely, the thermal resistance of the heat sink to the air, R_{hs}, the spreading resistance in the base, R_{sp}, and the thermal interface resistance, R_{TIM}. Each of these resistances have to be considered during the design process.

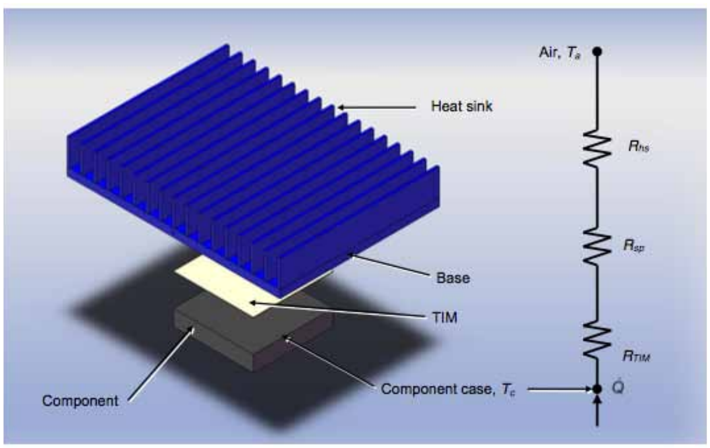

Figure 1. Exploded View of a Straight Fin Heat Sink and Equivalent Thermal Resistance Diagram

One also needs to look beyond the heat sink, to inside the component (if possible) and to the system level. Depending on the application, chassis or room level also needs to be looked at. The two aforementioned are shown graphically in Figure 2.

Figure 2. Thermal Analysis Chain of an Electronic System, From IC to Data Centre [2].

Apart from heat sink convective and radiative heat transfer optimization, key issues in advancing the effectiveness of air-cooling solutions include:

- Integrated circuit (IC) design and layout
- Package material development
- Die-to-die carrier and component-to-heat sink interface thermal contact resistance minimization, which can be comparable to the actual heat sink thermal resistance
- Integration of heat spreading technologies, such as heat pipes and high thermal conductivity materials, to minimize heat sink base temperature rise
- Aerodynamic fan performance improvement
- Integration of hybrid cooling solutions, such as phase change materials (PCMs) to manage peak transient heat loads
- Airflow optimization
- Minimization of heat sink surface fouling, whose impact on thermal resistance is becoming a major warrantee issue in both notebook and desktop computer products

- System architecture-based thermal management techniques
- Thermal load monitoring
- Sustainability
- Standardization of thermal management hardware performance characterization.

Heat Sink Manufacturing Technologies

Heat sinks function by extending the surface area of heat dissipating surfaces through the use of fins. Their design and analysis is one of the most extensive research areas in electronics cooling. Advances in heat sink cooling performance have been achieved through progress in manufacturing technology (Figure 3 and Table 1) and to a lesser extent, fan design, thereby resulting in more efficient heat removal from a given volume. Heat sink manufacturing technologies have been discussed in detail in past Qpedia articles [3].

Parameter	Extruded	Die-casting	Bonding	Folding	Modified Die-casting	Forging	Skiving	Machining
Min. t [mm]	1	0.175	0.75	0.25	0.2	0.4	0.3	0.5
Max. H/s	8:1	6:1	60:1	40:1	--	50:1	25:1	50:1
Min. s [mm]	6.6	8.3	0.8	1.25	0.2	1	2	1
Material	Al	Al, Zn-alloy	Al, Cu, Mg	Al, Cu	Al, Zn-alloy	Al	Al, Cu	Al, Cu, Mg

Table 1. Manufacturability Constraints: Innovative Versus Conventional Manufacturing Technologies, Compiled For A Range Of Heat Sink Suppliers [4].

Figure 3 (a) shows two types of extruded heat sinks, namely, straight fin and maxiFLOW™ heat sink types. Figure 3 (c) shows a copper skived heat sink with an integrated fan and spring loaded stand-offs.

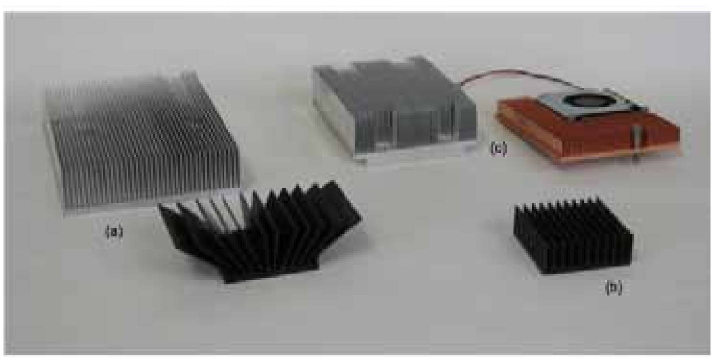

Figure 3. Some Heat Sink Manufacturing Technologies, Showing Extruded Heat Sinks (A), Forged Pin Fin (B) And Skived Aluminium And Copper Heat Sinks (C).

Heat Sink Fin Field Optimization

In the past, publications have focused on the parametric optimization of a heat sink thermal and hydraulic performance for a given application [1]. Despite the value of the publications, the optimization is limited to the case studied. For natural convection, Elenbaas [5] developed convective analysis using parallel plate Nusselt-Rayleigh number correlations. This work was extended to U-channel geometries representative of fin array heat sinks by Starner and McManus [6], Van de Pol and Tierney [7] and Aihara and Maruyama [8]. Ellison [9] derived a gray body radiative heat transfer analysis for these geometries.

Least energy optimization of a heat sink is a methodology that minimizes the energy consumed during manufacture and the operating costs while maximizing the thermal energy that can be extracted from the heat sink given the physical constraints. The physical constraints include the overall heat sink dissipation, heat sink material, manufacturing process and heat sink volume. The least energy optimization is presented by Kern and Kraus [10] to the optimization of a passively and actively cooled fin array heat sink design for manufacturability.

The least energy optimization method was followed by the minimization of entropy generation associated with the heat transfer and fluid friction [11], [12] and [13]. The least energy optimization and entropy have combined to form a phenomenological understanding of heat sink design optimization, in terms of cooling capability versus energy invested in the fabrication and operation of the heat sink.

Interface Thermal Resistance Minimization

In current high-performance air-cooled heat sink applications, the component-to-heat sink interfacial contact thermal resistance can be comparable to that of the actual heat sink [13]. Consequently, improved thermal interface materials are now the focus of much on-going research [13] [14] [15]. Thermal interface material (TIM) applications are categorized as TIM 1 and TIM 2, as shown in Figure 4. The aforementioned encompass a variety of adhesives, greases, gels, pads and PCMs. Recent advances in thermal interface technology include high-performance die attach materials and solder-based TIMs. A past Qpedia article [16] discussed the different types of TIM available, their specific applications and relative performance.

The bulk thermal conductivities of newly developed silver-filled or carbon fiber-loaded epoxy resin die attach adhesives, which are intended for high-performance/power ICs, are claimed to exceed those of eutectic solders. However, to fully exploit the potential of such materials, the die attach assembly process (adhesive deposition, curing) requires careful optimization to ensure good structural integrity of the bulk adhesive (maximum surface area coverage, minimum voiding) and optimum bondline thickness [14].

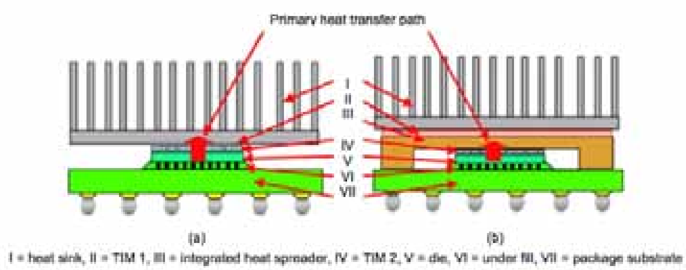

Figure 4. Thermal Architecture Typically Used (a) Laptop Applications, (b) Desktop And Server Applications [15].

Mechanical attachment

Mechanical attachment of a heat sink is not only used for the attachment of the heat sink to the component or system, but it is also an integral part of the heat sink design. This is because of the interface pressure required for the proper application of the interface materials. Attachment methods include thermally conductive tapes, epoxy, z-clips, component clip-ons, push pins with compression springs, spring load push pins and standoffs. Each has its own advantages and disadvantages, which have been discussed in detail in a Qpedia article [18].

Heat Spreading

A localized heat source acting on a heat sink base can generate significant spatial temperature gradients, as illustrated in Figure 5. The definition and control of thermal resistance has been discussed in detail in previous Qpedia articles [19] and [20]. Heat sink base thermal spreading resistance can be reduced through the use of highly thermally conductive materials, such as graphite or two-phase passive heat pipe heat spreading technology [21].

The two-phase heat transfer mechanism results in heat transfer capabilities from ten to several thousand times that of an equivalent piece of copper. Such as in heat pipes and vapour chambers shown in figure 6 [22]. A prior Qpedia article [23] discusses a comparison of thermal resistance of copper, silicon and heat pipes.

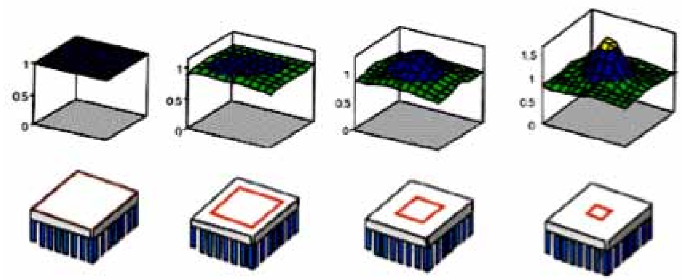

Figure 5. Heat Spreading On A Heat Sink Base: Normalized Local Temperature Rise With Heat Sources Of Different Size; From Left To Right, Source Area = 100%, 56%, 25%, 6% Of Heat-Sink Area [24].

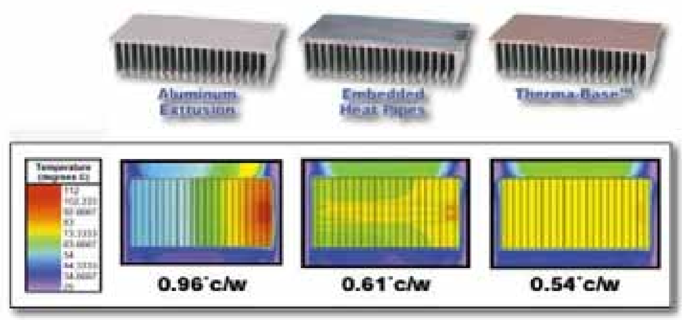

Figure 6. Heat Pipe Versus Vapor Chamber Thermal Performance Comparison [Thermacore].

Fan Performance

When selecting a fan for the cooling of a heat sink, it is essential to keep in mind that the system curve of the fan was determined in an idealised situation. When applied in an electronics cooling environment, the system can significantly differ from that is specified by the manufacturer. This has been previously discussed in a Qpedia article [25], where Figure 7 and Figure 8 show the reduced system curve for specific applications.

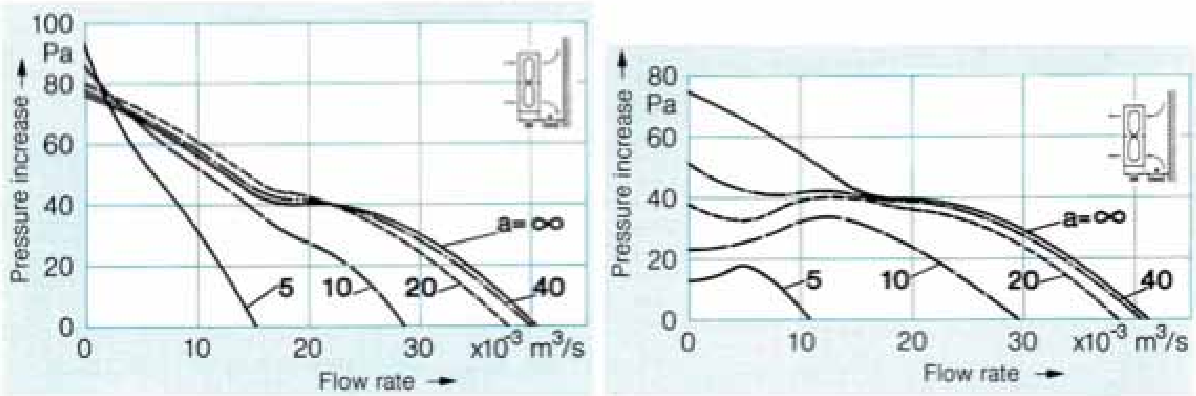

Figure 7. Change In The Characteristic Curve Of An Axial Fan Caused By A Square Plate On The Pressure Or Suction Side [26].

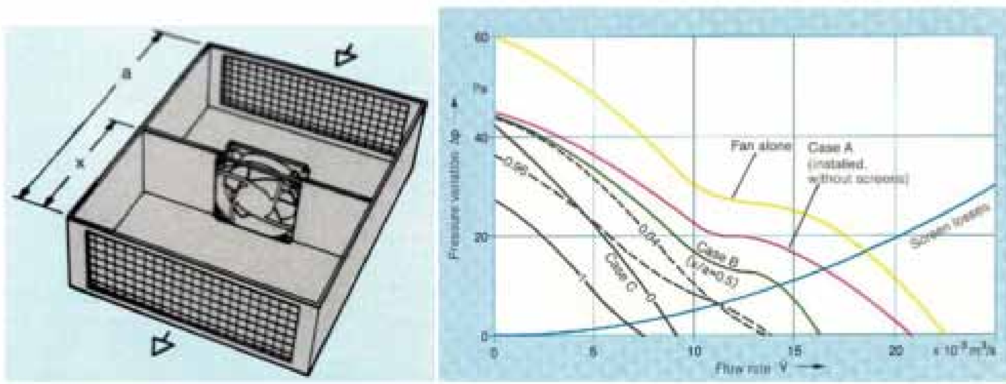

Figure 8. Fan Curve Performance As A Function Of Fan Placement [26]

Phase Change Materials (PCMs)

Thermal designs are typically focused on getting the absolute temperature below a certain maximum value for a design's continuous operation [27], based on worst-case assumptions [28]. In the peak loads, the temperature will rise towards the maximum allowed temperature. How rapidly will it rise depends on the thermal capacitance of thermal design. The thermal capacitance of a system can be increased by changing materials or by increasing the material available. Changing from an aluminium heat sink to a copper heat sink is an example of changing materials to increase the thermal capacitance of a heat sink. Both of the previously mentioned methods have direct cost implications. Copper is more expensive than aluminium and heavier. An alternative might be the use of phase change materials.

Going over an absolute maximum temperature is not the only means of failure for an electronics product. Thermally induced stress can cause cracking or delamination near the interface area of composites having different thermal expansion coefficients material properties. A means of reducing the temperature cycles can also be achieved by employing phase change materials in the design.

Surface Fouling

With the reduction of heat sink thermal design margins, which has resulted from rising processor heat dissipation, system miniaturization and fan acoustic noise constraints, the impact of fouling (9) on heat sink thermal resistance (thermal and hydraulic performance) has become much more critical than in the past. This impact is most pronounced for fine- pitch heat sinks, which are commonly employed for computer cooling. The resulting loss of heat sink cooling makes air-cooled desktop computers prone to self-protection shutdown, even in standard office environments. To maintain product performance and reliability, methods of minimizing heat sink fouling, such as anti-dust accumulating heat sink design features and filter design, require investigation. This will require an understanding of the mechanisms of heat sink fouling and its impact on thermal performance, as a function of contaminant and application environment, for a range of fine-pitched heat sinks.

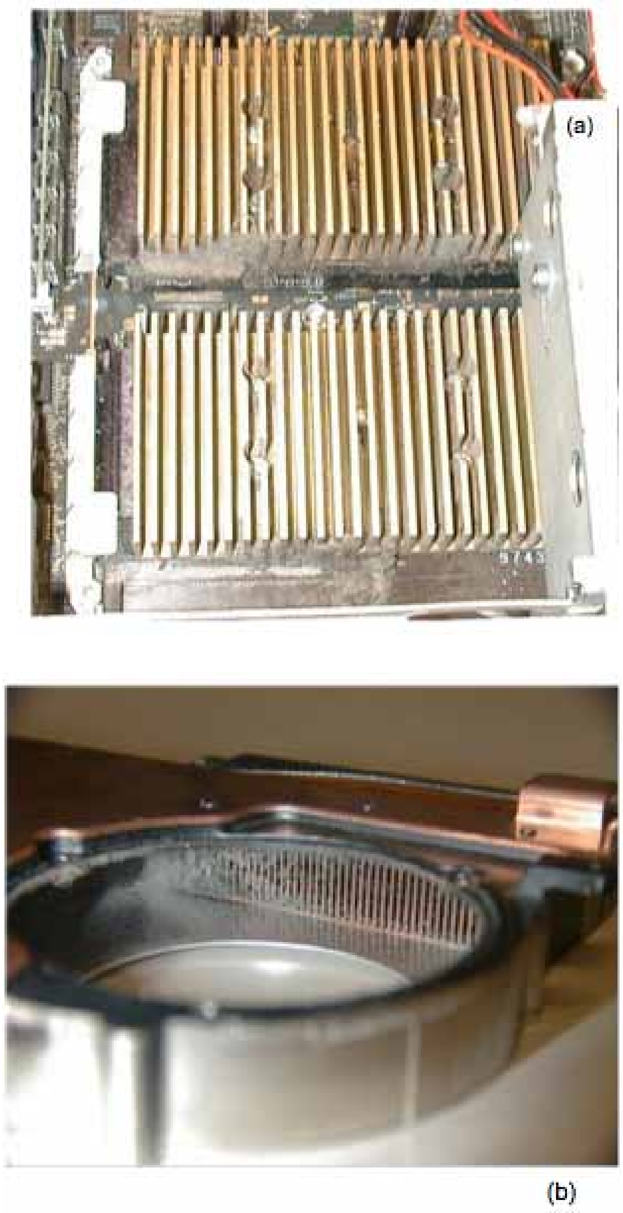

Figure 9. Heat Sink Fouling [Courtesy Of David Moore, HP]. (A) Desktop Application And Notebook Computer Application (B)

The article has discussed the various design parameters which will influence the effectiveness of the end heat sink design, ranging from heat spreading, fan performance to heat sink surface fouling. Even though a heat sink looks like a simple piece of metal, its implementation in a real application requires the information and knowledge of many different parameters in order to fully utilize the advantage of a heat sink.

References:
[1] Rodgers, P, Eveloy, V and Pecht, M.G., "Limits of Air-Cooling: Status and Challenges," in 21st IEEE Semi-Therm Symposium, 2005.
[2] Mahajan, R., Nair, R., Wakharkar V., Swan, J., Tang, J., and Vandentop, G., "Emerging Directions For Packaging Technologies," Intel Technology Journal – Semiconductor Technology and Manufacturing, Volume, 6 Issue 02, pp. 62 – 75, 2002.
[3] ATS, "Heat sink manufacturing technologies," Qpedia Thermal Management e- Magazine, Nov., 2010.
[4] Iyengar, M. and Bar-Cohen, A.,"Design for Manufacturability of SISE Parallel Plate Forced Convection Heat Sinks, IEEE Trans. Components and Packaging Technologies, Vol. 24, No. 2, pp.150-157, 2001.
[5] Elenbaas, W., "Heat Dissipation of Parallel Plates by Free Convection," Physica IX, No. 1 (1942), pp. 1-28.
[6] Starner, K.E. and McManus, H.N., "An Experimental Investigation of Free Convection Heat Transfer From Rectangular Fin Arrays," Trans. ASME, Journal of Heat Transfer, pp. 273-278, August 1963.
[7] Van de Pol, D., and Tierney, J., "Free Convection Heat Transfer from Vertical Fin Arrays," IEEE Trans. Parts, Hybrids and Packaging, Vol. PHP-10, No. 4, pp. 267-271, 1974.
[8] Aihara, T., and Maruyama, S., "Optimum Design of Natural Cooling Heat Sinks with Vertical Rectangular-Fin Arrays," Proc. Int. Symp. on Cooling Technology for Electronic equipment, Honolulu, Hawaii, pp. 35-54, 1998.
[9] Ellison, G.N., "Generalized Computations of the Gray Body Shape Factor for Thermal Radiation from a Rectangular U-Channel," IEEE Trans. Components, Hybrids and Manufacturing Technology, CHMT-2, No. 4, pp. 517-522, 1979.
[10] Kern, D. and Kraus, A., "Extended Surface Heat Transfer," McGraw-Hill (New York, 1972).
[11] Culham, J.R. and Muzychka, Y.S., "Optimization of Plate Fin Heat Sinks Using Entropy Generation Minimization," IEEE Trans. Components and Packaging Technologies, Vol. 24, No. 2, pp.159-165, 2001.
[12] Bar-Cohen, A. and Iyengar, M., "Least-Energy Optimization of Air-Cooled Heat Sinks for Sustainable Development," IEEE Trans. Components and Packaging Technologies, Vol. 26, No. 1, pp. 16-25, 2003.
[13] Nakayama, W., and Bergles, A.E., "Thermal Interfacing Techniques for Electronic Equipment - A Perspective," Trans. ASME, Journal of Electronic packaging, Vol. 125, No. 2, pp. 192-199, 2003.
[14] Mukadam, M., Schake, J., Borgesen, P., Srihari, K., "Effects of Assembly Process variables on Voiding at a Thermal Interface," Proc. Ninth Intersociety Conference on Thermal and Thermomechanical Phenomena in Electronics Systems (ITHERM), Las Vegas, Nevada, USA, June 1-4, pp. 58-62, 2004.
[15] Mahajan, R., Chiu, C.P., and Prasher, R., "Thermal Interface Materials: a Brief Review of Design Characteristics and Materials," Electronics Cooling, Vol. 10, No. 1, 2004.
[16] ATS, "Decreasing thermal contact resistance by using thermal interface materials," Qpedia Thermal Management e-Magazine, Aug., 2008.
[17] Van Heerden, D., Rude, T., Newson, J., Knio, O., Weihs, T.P., Gailus, D.W., "Thermal behaviour of a soldered Cu-Si interface," Twentieth Annual IEEE Semiconductor Thermal Measurement and Management Symposium, pp 46-49, 2004.
[18] ATS, "Heat sink attachment options," Qpedia Thermal Management e- Magazine, Jul., 2008.
[19] ATS, "Spreading resistance; Its definition and control," Qpedia Thermal Management e-Magazine, Sep., 2010.
[20] ATS, "Spreading resistance of single and multiple heat sources," Qpedia Thermal Management e-Magazine, Aug., 2007.
[21] Soule, C.A., "Future Trends in Heat Sink Design, Electronics Cooling, Vol. 7, No. 1, 2001.
[22] Katoh, T., Xu, G., Vogel, M., and Novotny, S., "New Attempt of Forced-Air Cooling for High Heat-Flux Applications," Proc. Ninth Intersociety Conference on Thermal and Thermomechanical Phenomena in Electronics Systems (ITHERM), Las Vegas, Nevada, USA, June 1-4, pp. 34-39, 2004.
[23] ATS, "Heat spreading with copper, silicon and heat pipes," Qpedia Thermal Management e-Magazine, Nov., 2010.
[24] Lee, S., "Calculating Spreading Resistance in Heat Sinks," Electronics Cooling, Vol. 4, No. 1, 1998.31 Lopatinsky, E. and Waldman, M., "Recognizing the Limits of Conventional Axial Hub-Motor AHS Devices," Electronics Cooling, Vol. 9, No. 3, 2003.
[25] ATS, "How Baffles and Plenumns Affect Fan Performance," Qpedia Thermal Management e-Magazine, Apr., 2009.
[26] Harmsen, S., "Equipment Fans for Electronic Cooling: Function and Behaviour in Practical Application, verlag moderne industrie, 1991.
[27] Parry, J.D., Rantala, J., and Lasance, C.J.M., "Enhanced electronic system reliability – challenges for temperature prediction," IEEE Trans. on Components and Packaging Technologies, vol. 25, no 4, pp. 533-538, 2002.
[28] Skadron, K., "A computer-architecture approach to thermal management in computer systems: challenges and opportunities," in Proc. Fifth International Conf. on Thermal and Mechanical Simulation and Experiments in Micro-Electronics and Micro-Systems (EuroSimE), Brussels, Belgium, May 9-12, pp. 415-422, 2004.

Spray Cooling Electronics

in a 1-U Chassis

When it comes to designing electronics for a Navy submarine, efficient use of space and power are high on a long list of requirements. Electronics and their cooling systems must also pass tough environmental tests, including operation in temperature extremes, at different pressures and humidity levels, and survivability through shock, vibration, and temperature swings. On top of that, electronics racks in submarines are not as deep as standard racks.

These strict requirements have typically precluded the use of the state-of-the-art components in military electronics, simply because they dissipate too much heat. When it comes to the highest performing processors, air cooling can't cool well enough at the elevated temperatures, the fans use too much power and would not meet noise requirements, or it may not fit into the required space.

Isothermal Systems Research (Now known as SprayCool) developed a recirculating liquid spray cooling system that utilizes two-phase cooling, where a dielectric liquid is sprayed onto a heated surface and some of the fluid boils as it absorbs heat [1]. Named the SprayCool Compact Server (SCS), a high performance dual-processor motherboard and the entire spray cooling system are able to fit into a 1-U rack height housing with shallow depth. Shown in Figure 1 below, the cooling system is quite compact, with a small heat exchanger and a coolant reservoir with an integrated pump. The spray modules which cool the CPUs use the same mounting as the standard air cooled heat sinks.

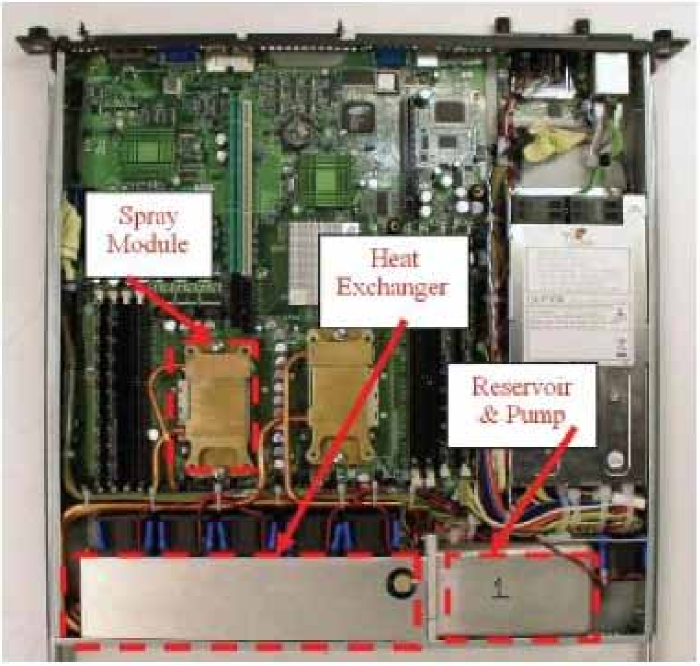

Figure 1. ISR SprayCool Compact Server [1]

ISR opted to use two-phase spray cooling rather than straight liquid cooling with a cold plate, because the heat exchanger would have been much larger. The required flow rate would also have been much higher; cooling systems that are available for high-end computers use flow rates that are 5 to 25 times greater than that used in the SCS. The smaller flow rate means that a smaller pump may be used, and less power will be used for coolant circulation.

The fluid flow can be greatly reduced in a two-phase cooling system because a given liquid absorbs much more energy than simply raising the temperature of that liquid several degrees when it changes phase from liquid to gas. In experiments, Marcinichen and Thome found that a single-phase water cooling system needed about 10 times more flow rate than a two-phase cooling system based on R134a [2]. Aside from using a smaller pump, reductions in tubing and other flow-related hardware sizes can use less space as well.

In addition, the component cooler can be smaller. An example of a typical active heat sink found in an HP rx2600 server compared to an ISR spray module can be seen in Figure 2. In some applications, the heat exchanger, reservoir and pump would occupy additional space, but for many server applications, an external coolant system can be used to cool multiple servers [3].

Figure 2. Traditional Active Heat Sink (left) Compared to ISR Spray Module [3]

ISR tested three different processors in the SCS and in an equivalent air cooled chassis. Of the processors, the single core Intel Xeon 3.6GHz had the highest power rating, at 103W. With air cooling, the CPU temperatures could only be kept within manufacturer's specifications in up to 5ºC ambient temperature. The SCS was able to remove much more heat, and could operate in 33ºC ambient temperatures with the same CPU temperatures. The results are shown in Figure 3. Note that both processors are at the same temperature when spray cooled.

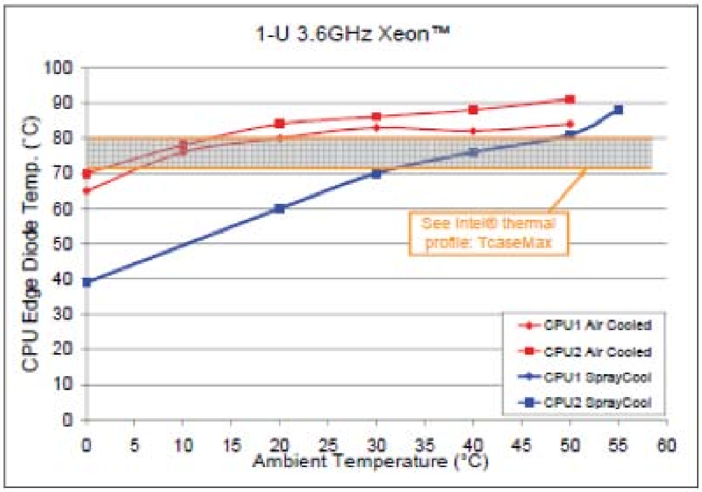

Figure 3. Xeon CPU Temperature, Air Cooling vs. SprayCool [1]

Above those temperatures, the CPUs would continue to operate, but at a lower performance level. The performance of the air cooled server began to fall off at around 10ºC ambient temperature, while the SCS maintained full performance until over 30ºC. The performance vs. ambient temperature curve is shown in Figure 4. The relative performance score of 100% is defined as the performance of the server on benchmark tests when air cooled at 0ºC ambient.

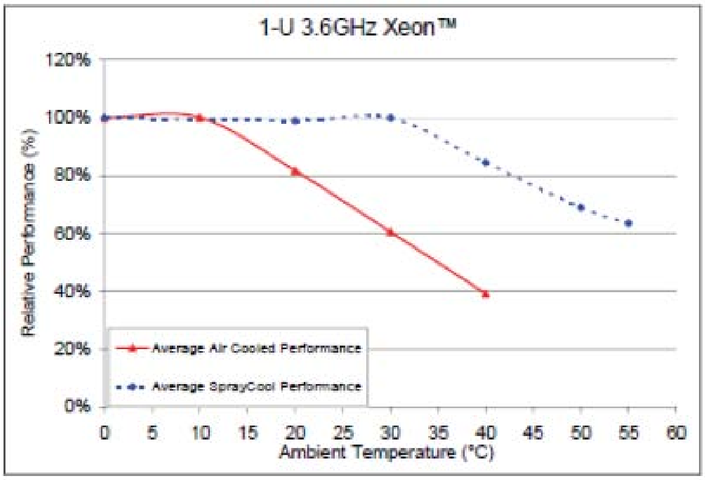

Figure 4. Server Performance vs. Ambient Temperature [1]

The overall server power consumption, which included the cooling system, was slightly more complicated because the CPUs used less power when they throttled back performance. At most ambient temperature conditions, the air cooled server used less power than the SCS, apparent in Figure

5, but it should be noted that the server performance was much better for the SCS. It could be argued that the SCS cooling system is more efficient than air cooling because the SCS server uses less power at 0ºC ambient, when both systems are operating at full performance.

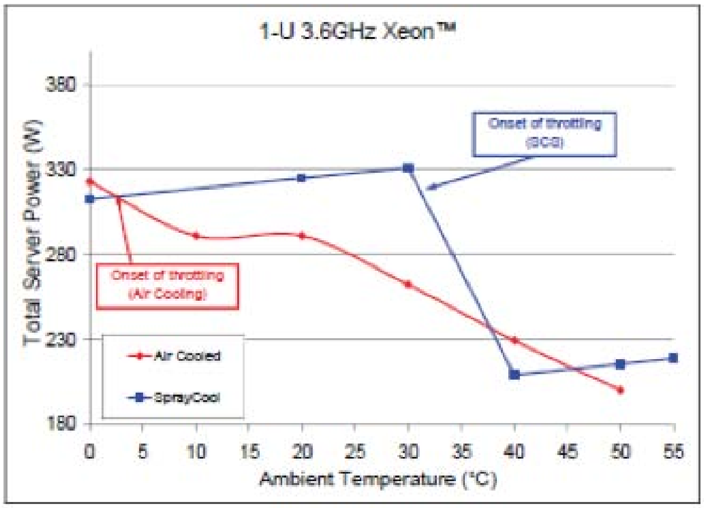

Figure 5. Overall Server Power Consumption vs. Ambient Temperature [1]

Cader et al. saw significant power savings when they applied the SprayCool system in a datacenter. For a full rack of HP rx2600 servers, a net energy savings of 330W was observed [3]. For an entire data center, this could translate to a reduction of tens of thousands of watts. In addition, with the SprayCool system transferring heat directly to a chilled water supply rather than the ambient air, the need for air conditioning could be reduced drastically.

With reduced power consumption, compact size, and improved processor cooling, spray cooling systems appear to be viable alternatives to air cooling for use on military ships. ISR's SCS passed all of the required military testing, and did not fail until it was exposed to 100ºC operating temperatures. The strong cooling performance allowed many off the shelf components to be used in the design, including the commercially available CPUs, which helped to keep costs down. For all these reasons, spray cooling and other advanced thermal management techniques will undoubtedly be seen more and more in demanding applications.

References:

1. Johnston, A.D., Stone, D.L., Cader, T., Locklear, D.A., "SprayCool Compact Server for military shipboard environments," Isothermal Systems Research Inc., 2007. 2. Marcinichen, J.B., Thome, J.R., "New Novel Green Computer Two-Phase Cooling Cycle: A Model for Its Steady-State Simulation," in ECOS2010, Lausanne, Switzerland, 2010.

3. Cader, T., McAllister, H.J., Westra, L., Marquez, A., Regimbal, K.M., Seim, T.A., "Energy Smart Data Center (ESDC) Final Report," Pacific Northwest National Laboratory, Richland, WA, 2005.

SHORTCUTS CAN BE RISKY!

REMOVE UNCERTAINTY. GO TO MARKET FIRST. AVOID RECALLS.

Work with trusted advisors with 150 years of collective thermal management experience and innovative thinking. Benefit from their advanced testing facilities and best practices.

ATS ADVANCED THERMAL SOLUTIONS, INC.
Innovations in Thermal Management®

From consulting to custom designs, ATS takes the risk out of decision-making. Call us today at 781.769.2800, email sales@qats.com or click the QR symbol for our website

Transient Response of a PCM

with Embedded Graphite Nanofibers

In electronics cooling, there are several options when choosing how to leverage the latent heat characteristics of a phase change material. Considerations are made to accommodate manufacturing, workability, and thermal performance. Reliability issues have forced thermal engineers to suspend the pursuit of active cooling options such as heat pipes, and persist toward innovative methods in passive cooling solutions. Great strides have been made in the application of phase change materials embedded with graphite nanofibers to improve the transient thermal response.

The ability to store and dissipate heat energy with phase change material (PCM) dates back to the refrigerated rail car. Today, phase change materials are used in NASA spacesuits, home insulation and clothing such as the modern "long john." Harnessing this technology has benefitted thermal cooling solutions for many years and Figure 1 shows how a phase change material absorbs heat energy during a phase change and then dissipates it when changing back, as happens when using a heat pipe. With an internal wick, the heat pipe is filled with a liquid with a high latent heat. The liquid heats up enough during operation and vaporizes storing that heat energy, and travels via open channel to a cooler region where it changes back into a liquid, releasing the heat energy where it can be easily dissipated. Driven by capillary force, the liquid travels back to the hot side through a wick.

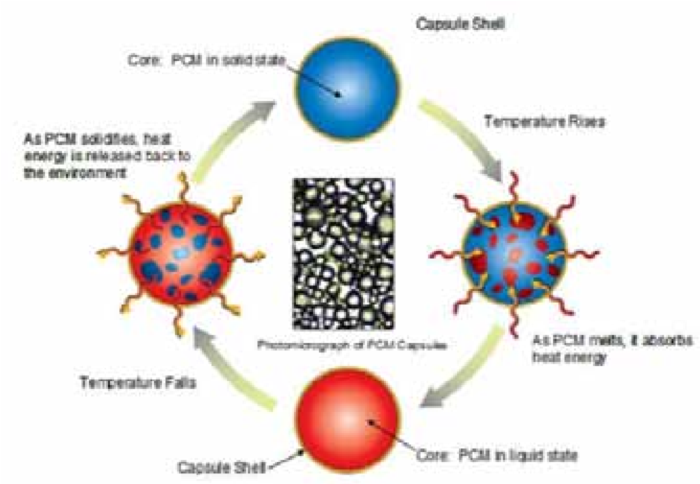

Figure 1. Phase Change Cycle [3]

For heat sink applications, where pressure can be applied to the PCM during installation and operation, PCM may be the better choice TIM when compared to the alternatives. Having the consistency such as toothpaste encapsulated within a flat coupon enables PCM to replace gap pads and grease. The PCM naturally flows into the surface irregularities of components and heat sinks as the assembly is heated. They provide simple assembly, low thermal resistance and energy storage properties as they reach their melting point. Latent heat by definition is the heat required to convert a solid into a liquid (for this application) at a constant temperature. Latent heat storage is one of the most efficient ways of storing thermal energy. Unlike the sensible heat storage method, the latent heat storage method provides much higher storage density, with a smaller temperature difference between storing and releasing heat [5]. Figure 2 is a representation of the temperature rise through a phase change, and shows the relationship between sensible heat, where the temperature rises linearly, and latent heat, where temperature maintains constant as the energy is used to overcome the attractive forces between molecules.

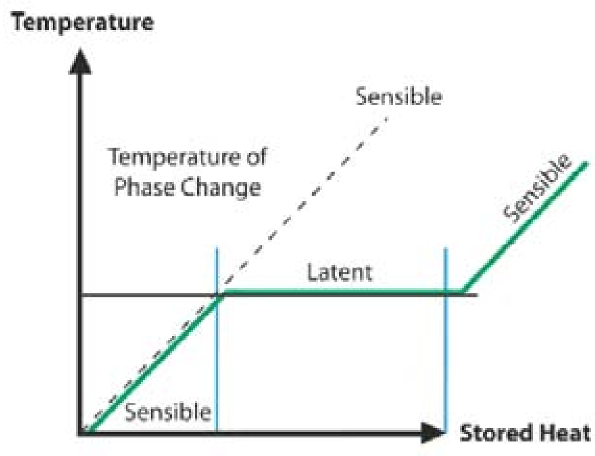

Figure 2. temperature rises vs. stored heat through a phase change

High-resolution transmission electron microscopy studies have revealed that the nanofibers consist of extremely well-ordered graphite platelets which are oriented in various directions with respect to the fiber axis. The arrangement of the grapheme layers can be tailored to a desired geometry by choice of the correct catalyst system and reactions conditions [2]. During the process, the graphite precipitates in the form of parallel basal planes, which may take the forms shown in Figure 3.

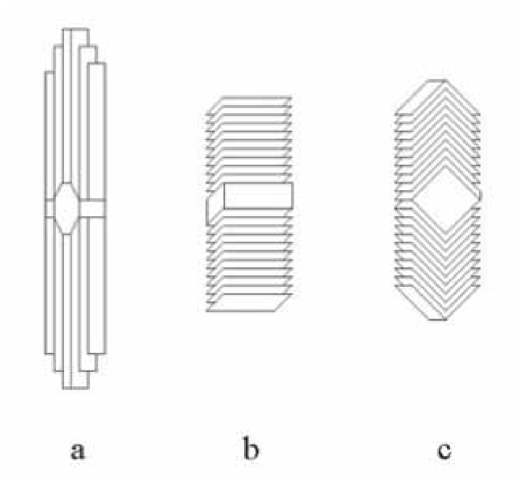

Figure 3. GNF Styles (a) platelet (b) ribbon (c) herringbone [1]

Paraffin waxes have been widely studied as PCMs because of their high latent heat, but due to their low thermal conductivity, bottlenecking of the heat flow occurs as well as isolation of the melt process near the heat source. Today, you will see PCMs encapsulated in a higher conductivity material, such as aluminum, to more evenly distribute the heat flow, which of course leads to higher effectiveness. Furthermore, the PCM is enclosed within a sealed module so that it doesn't contaminate the device as it melts [1]. As covered in our June, 2011 edition of Qpedia, you can read up on other thermal management technologies such as foams and heat spreaders embedded with PCM. There are disadvantages when these technologies are deployed in high power electronics such as added weight, and manufacturing limitations.

Graphite nanofibers (GNF) are a type of material that is produced by the decomposition of carbon containing gases over metal catalyst particles at temperatures around 600ºC.

The work at Villanova University investigates the transient response of a fixed volume paraffin wax PCM with embedded GNF of these three various styles at different loading levels and compares them to the transient response of the base PCM. The apparatus used is a cube with walls of low thermal conductivity, a copper alloy base which is heated, and a cold plate as a top, circulating 50/50 water and antifreeze maintaining a temperature of 5ºC.

The study's expectations of the base PCM embedding with GNFs are to:

- Heat more quickly and uniformly to the PCM melt temperature.
- Remain at the PCM melt temperature for an extended period, taking advantage of the energy storage characteristics of the phase change process.
- Achieve a lower steady state temperature at, or slightly above, the PCM melt temperature.

During testing, the temperature rise was monitored with thermocouples after reaching the PCM melting point. As suspected, the steady state temperatures of the mixtures fall below that of the base PCM. Figure 4 shows the temperature and time response of each style PCM/GNF of 0.25wt% mixture and its relationship to the base PCM under a power load of 7W.

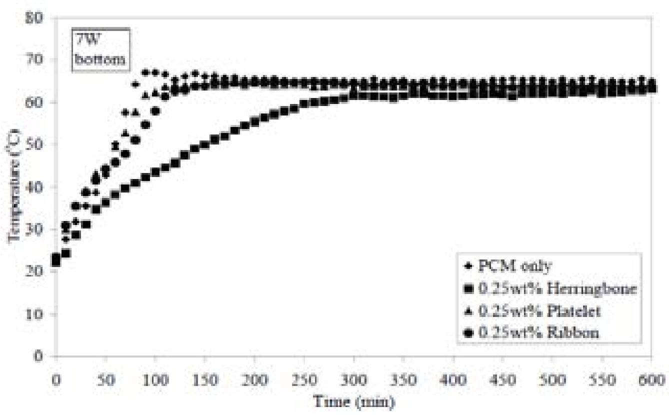

Figure 4. Transient Thermal Response PCM Styles with GNF of 0.25wt% [1]

All three mixtures exhibit a reduction in steady-state temperature, as compared to the base PCM and, as has been shown in the other results, herringbone mixtures are slower than the ribbon and platelet mixtures in their thermal response. When monitoring the PCM/GNF mixtures at a greater distance from the heat source, the platelet and herringbone mixtures fail to melt completely, which indicates that this PCM/GNF mixture could operate effectively under a higher heat load. Testing higher GNF levels have been found to increase the PCM viscosity during the liquid phase, which influences, and, in some cases, suppresses the development of the Rayleigh- Benard convection currents that occur after the PCM reaches its melting point. [1]

The motivation behind this article was to show how the use of graphite nanofibers has improved the performance of basic PCMs for use in electronic cooling applications. While this study showed that the GNF/PCM mixtures of 0.25wt% exhibits a reduction in steady-state operating temperatures, as compared to the base PCM, it was also found that high GNF loadings increased viscosity and reduced the convection currents within the mixtures and led to overheating the PCM. It may yield improvements to these PCMs by further testing to find the optimal GNF loading levels for each GNF style. All TIMs perform better with increased pressure applied; unfortunately, datasheets currently don't reflect pressures used in real world applications. In a future Qpedia article, a comparative testing will compare standard PCMs, thermal tapes and gap pads under similar operating conditions for industry professionals to use when assembling an engineered cooling solution.

References:

1. Kopec, T. et al., "Transient thermal performance of phase change materials with embedded graphite nanofibers" 2007

2. Park, C. et al., "Hydrogen storage in graphite nanofibers" 1998

3. Microtek laboratories, "Encapsulated PCMs: How They Work" 2010 4. Zang, Ya Nan et al., "Energy Storage Properties of Phase Change Materials Prepared from PEG/CPP" 2004

Cooling News

New Products, Services and Events from around the Industry

High Thermal Conductivity Composite Material

Rogers RT/duroid® 6035HTC high frequency materials are ceramic filled PTFE composites for use in high power RF and microwave applications. With a thermal conductivity of almost 2.4 times the standard RT/duroid 6000 products, and copper foil with excellent long term thermal stability, RT/duroid 6035HTC laminates are an exceptional choice for high power applications. Rogers advanced filler system enables excellent drillability, reducing drilling costs as compared to standard high thermally conductive laminates which use alumina fillers.

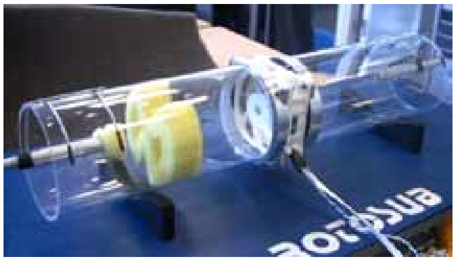

World's First Self Silencing Fan

Noise pollution from fans has always been a problem. The novel RotoSub technology, RotoSub R-ANC, takes a completely new approach by addressing the problem at its source, enabling the fan to reduce its own noise. RotoSub R-ANC is an active noise reduction solution that integrates fully into the fan itself. The solution dramatically reduces its noise without increasing the size of the fan or requiring any additional components.

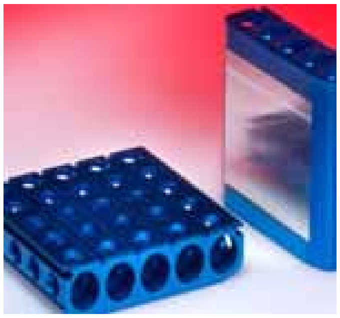

Honeycomb Heat Sink

JaroThermal's newest Honeycomb heat sink directs heat towards the outside, while producing a steady flow of cool air on the inside. Thanks to a multi-holed design and increased surface area, the Honeycomb optimizes cross ventilation, while simultaneously cooling the surrounding ambient air. Applications include a wide range of cooling solutions for video cards, motherboards and networking applications. JARO's adhesive mounted version eliminates the need for mounting holes in the PC Board.

Chip Coolers

The AP 5008 is one of a series of chip coolers from ADDA designed to cool high-power, on-board components such as accelerator cards. With a frame size of 50 x 50mm and a profile of only 8mm, the AP 5008 is available in three speed options and produces an airflow of 3.4 liters/second (7.2CFM) at a power rating of 0.5W. All blowers in the ADDA AP range have air outlets on all four sides of the fan frame to allow ventilation over a wide area, and the high performance ADDA eight-pole motor design ensures high reliability and long life. They operate from a 5V or 12V supply and are RoHS compliant. They are built in frame sizes of 35, 40, 45, 50 and 52mm with profiles of 8, 10 and 12mm.

Liquid Cooling Package

Blade and 1U servers are leading to climate control problems in racks and subsequently changing the requirements of the IT infrastructure. Matching cooling capacities to present and future demand is crucial and Rittal's new LCP Extend (liquid cooling package) unit is based on an air/water heat exchanger which solves the problem of high heat losses of up to 12 kW per rack.
Without having to modify an existing series of enclosures, the innovative package can be attached as an independent cooling unit to the rear doors of practically any rack, while the rack is in operation. This means that the system can be easily retrofitted in the event of any problems resulting from thermal issues.

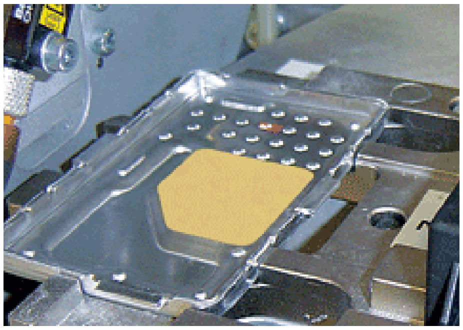

Thermal Phase-Change Material for High-Power Devices

Designed for use with a high-power electrical device requiring electrical isolation from the heat sink, Bergquist's High Flow 650P thermally-conductive phase change material is reinforced with a polyimide film. Naturally tacky on one side, the film offers a 5,000-Vac dielectric breakdown voltage, thermal conductivity of 1.5 W/m-K, and a thermal impedance of 0.20°C-in2/W at 25 psi. The material is reliable in temperatures to 150°C. It is available in standard thicknesses of 0.0045-, 0.0050- and 0.0055-in. and with a 1.0, 1.5 or 2.0 mil polyimide reinforcement carrier.

Tools and Techniques for the Thermal Management of Small, Medium, and Large Scale Data Centers

Datacenters are effectively large scale systems whose components are racks of computers.
Novel approaches to cooling datacenters of various sizes are being undertaken today to obtain the best and most green cooling possible. This webinar will consider approaches for small, medium, and large scale datacenters to achieve a given datacenters cooling goals

October 27, 2011 2:00 p.m. (EST)

Tips, Tricks and Techniques for the Best Use of CFD for Heat Sink and System Modeling

Computational Fluid Dynamics (CFD) simulation software is an essential part of the thermal professional's tool box and often the starting point in the design of a thermal management solution. Proper CFD saves an engineer time and cost in a design. ATS will discuss general tips and tricks in working with CFD. The agenda includes the simplest methods of preparing a CFD model; the best techniques for meshing; and how to model a system's components, such as fans and perforated plates. Attendees will learn about common and not-so-common issues in CFD, and how to overcome them.

November 3, 2011 2:00 p.m. (EST)